Ion-induced kinetic electron emission from ^{6}LiF, ^{7}LiF and MgF_2 thin films*

S. Ullah[a)], A. H. Dogar[b)], M. Ashraf[c)], and A. Qayyum[b)†]

[a)] *Pakistan Institute of Engineering and Applied Sciences, Nilore, Islamabad, Pakistan*
[b)] *Physics Division, Pakistan Institute of Nuclear Science and Technology, P. O. Nilore, Islamabad, Pakistan*
[c)] *Optics Laboratories, P. O. Box 1021, Islamabad, Pakistan*

(Received 28 August 2009; revised manuscript received 18 January 2010)

Secondary electron yields for Ar^+ impact on ^{6}LiF, ^{7}LiF and MgF_2 thin films grown on aluminum substrates are measured each as a function of target temperature and projectile energy. Remarkably different behaviours of the electron yields for LiF and MgF_2 films are observed in a temperature range from 25 °C to 300 °C. The electron yield of LiF is found to sharply increase with target temperature and to be saturated at about 175 °C. But the target temperature has no effect on the electron yield of MgF_2. It is also found that for the ion energies greater than 4 keV, the electron yield of ^{6}LiF is consistently high as compared with that of ^{7}LiF that may be due to the enhanced contribution of recoiling ^{6}Li atoms to the secondary electron generation. A comparison between the electron yields of MgF_2 and LiF reveales that above a certain ion energy the electron yield of MgF_2 is considerably low as compared with that of LiF. We suggest that the short inelastic mean free path of electrons in MgF_2 can be one of the reasons for its low electron yield.

Keywords: ion-induced electron emission, alkali halides, electronic stopping, electron mean free path

PACC: 3450D, 7920N, 7960G

1. Introduction

The phenomenon of ion-induced electron emission from the surface of the solid is of genuine interest in fundamental research and plays an important role in many technological applications, for example, in the accurate measurement of ion currents, in particle detection, in surface analysis techniques and in plasma wall interactions. There are two known mechanisms of secondary electron emission, namely potential emission and kinetic emission. The potential emission of electron takes place if the potential energy of the ion exceeds twice the work function of the target. The kinetic electron emission results from the direct transfer of kinetic energy of incident ion to the target electron. The process of kinetic electron emission is usually described by a so-called three-step model.[1,2] These steps are as follows: (i) excitation of electrons in solid by kinetic energy deposition from incoming ions, (ii) transport of these electrons to the surface of the solid, and (iii) transmission of electrons through the surface into the vacuum. The relative importance of these steps has been separately analysed in theoretical studies but this separation is difficult in experimental studies. A typical parameter that describes the kinetic electron emission is the electron yield, γ, the number of electrons that are emitted per incident ion. According to the most frequently applied theoretical models,[3−5] γ should be proportional to the energy loss of the ion near the solid surface, i.e.

$$\gamma = \Lambda S_{\rm e}, \tag{1}$$

where Λ is a constant that depends on material properties like the mean energy required for producing free electron within solid, the mean free path of electrons in solid and the escape probability for electrons to overcome the surface barrier; $S_{\rm e}$ is the electronic stopping power. A great many of reliable data on the electron yields of metal targets with ions in low[6,7] and medium-to-high[8−10] energy ranges are available.

On the other hand, there are only a few studies on the non-metals that include some oxides[11−13] and alkali halides.[14,15] The reason is clear: the ion beam creates positive potential at the surface of the insulator, which prohibits the accurate measurement of electron yield. Nevertheless, the electron emission from insulators is an intriguing phenomenon, which is because, compared with metal, an insulator has completely different characteristics concerning the three steps involved in kinetic emission of electron. For in-

*Project partially supported by the Higher Education Commission of Pakistan through indigenous PhD program.
†Corresponding author. E-mail: qayyum@pinstech.org.pk
© 2010 Chinese Physical Society and IOP Publishing Ltd

stance, first, the large band gap of the insulator can suppress the electron excitation process, but there is no experimental evidence to support this idea; secondly, electrons have larger escape depths in insulators due to reduced electron scattering; thirdly, the insulators have lower surface barrier potential than metals. As opposed to the large band gap, large electron escape depth and lower surface barrier of insulator are in favour of a higher kinetic electron yield. Careful survey of the existing experimental result reveals that the kinetic electron yield of insulators is generally higher than that of metals. In this study, we measure secondary electron yields of ^{6}LiF, ^{7}LiF and MgF_2 thin films each as a function of target temperature and projectile energy. The measured electron yields of these films are discussed in the framework of the existing models to understand the kinetic electron emission process in insulators.

2. Experimental setup

Thin films of ^{6}LiF, ^{7}LiF and MgF_2 were deposited on aluminium substrates by a resistive heating technique, by using a high vacuum coating unit (Edward 610A). The aluminum substrates were first treated with detergent and washed in deionized water. The substrates were then dried with a fine tissue paper and cleaned with isopropyl alcohol (IPA) in an ultrasonic cleaner for 30 min. The vacuum better than 1×10^{-4} Pa was maintained in the chamber during deposition. The substrate was kept at room temperature ($\sim$ 25 °C) during deposition. The film thickness and the deposition rate ($\sim$1.20 nm/s) were monitored by quartz crystal thickness monitor FTM5. Thicknesses of the films were 500$\pm$10 nm. Structures of the films were determined by x-ray diffraction (XRD) at room temperature by Bruker D8 diffractometer using Cu K_α radiation in the scanning mode. The XRD profiles of ^{6}LiF, ^{7}LiF and MgF_2 films are shown in Fig. 1. ^{6}LiF and ^{7}LiF films are polycrystalline, each having a cubic structure (a = 4.046 and 4.045 Å, 1 Å = 0.1 nm respectively) with orientations along (111), (200), (220), (311) and (222) planes. MgF_2 film was also polycrystalline in nature, having a tetragonal structure ($a = b$ = 4.656, c = 3.059 Å) with orientations along (110), (111) and (211) planes. The target films were then mounted on a manipulator and brought one by one in front of the ion beam. Each film was sputter cleaned with a 5-keV Ar^+ beam for 10 min before the actual electron yield measurement. The electron yield was also monitored in the cleaning process. Initially the electron yield was unstable then it became reasonably stable after 10 min of sputter cleaning, indicating that surface contaminants have been removed. As the films were sputtered under similar conditions, we believe that damages induced in the films in the cleaning process are almost the same.

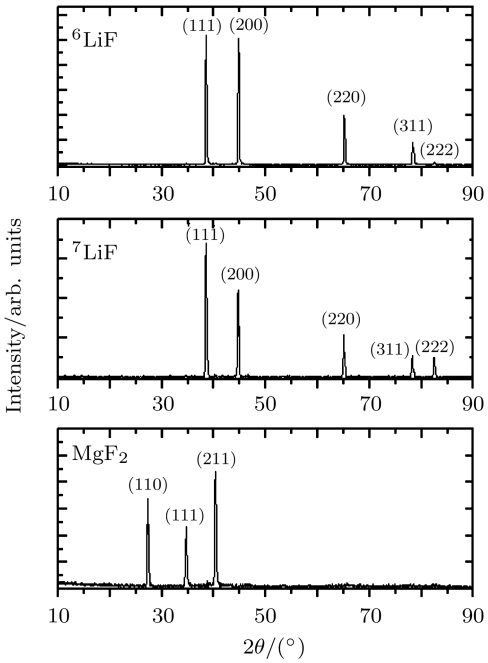


Fig. 1. XRD patterns of ^{6}LiF, ^{7}LiF and MgF_2 thin films.

The detailed description of the ion-beam system used in this study is given elsewhere.[16] Briefly, 2–10 keV Ar^+ ions produced from a duoplasmatron ion source were focused at the entrance aperture of $E \times B$ velocity filter by an Enzel lens. After charge and mass selection by $E \times B$ velocity filter, the ions were directed onto the target films that were placed inside a cage (see Fig. 2). The current density at the target surface was in a range of 15–40 μA/cm^2. The pressure in the target chamber was maintained at about 10^{-7} Pa by a 400-l/s Varian ion pump. Target films were placed perpendicular to the ion-beam direction in a cage (see Fig. 2). A beam defining collimator was used to prevent the incoming ions from directly impacting the forthcoming striping and rejection apertures and had a diameter of 2 mm. A potential of +100 V was applied to a beam defining collimator to minimize ion-induced emission of electrons from its edges. The striping aperture prevented ions scattered by the collimator from entering the target region. The striping aperture and the rejection aperture had diameters of 3 mm and 3.5 mm respectively. A cage

that was operated with a ±80-V square wave generator surrounded the target in order to collect or suppress electrons emitted from the target. The cage had an aperture of 4.5 mm for ion beam entrance, through which the incident ion beam collimated to 2 mm in diameter was able to reach the target surface. A rejection electrode at a potential of –100 V was placed before the cage that prevented electrons from escaping and thus further enhanced the electron collection efficiency. The current at the target was measured with a pico-ampere meter and then fed into a computer.

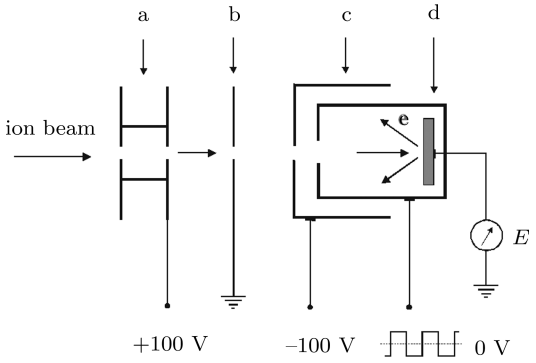


Fig. 2. Schematic diagram of the experimental setup used for secondary electron emission studies. (a) Beam defining collimator, (b) striping aperture, (c) rejection aperture, (d) cage and (e) Pico-Amperemeter.

When a voltage of +80 V is applied to the cage with respect to the target, the total current I_+ measured at the target consists of two components, i.e. the current of incoming ions, I_i, and the current of emitted electrons, I_e as given by

$$I_+ = I_\mathrm{i} + I_\mathrm{e} = I_\mathrm{i} + \gamma\,(I_\mathrm{i}/q)\,, \tag{2}$$

where q is the charge of incoming ion. Applying a voltage of –80 V to the cage leads to a target current I_- that is equal to the incoming ion current

$$I_- = I_\mathrm{i}. \tag{3}$$

Therefore, the total electron yield is given as[17]

$$\gamma = \frac{I_\mathrm{e}}{(I_\mathrm{i}/q)} = q\frac{I_+ - I_-}{I_-}. \tag{4}$$

3. Results and discussion

Secondary electron yields of ^{6}LiF and MgF_2 measured each as a function of target temperature for 8-keV Ar^+ impact are shown in Fig. 3. The indicated error bars show statistical error in the current measurements. For ^{6}LiF the electron yield sharply increases with temperature increasing and becomes almost constant after about 175 °C. The scatter and the decrease of electron yield observed below this temperature are due to the macroscopic charging of the target by the ion beam. Above 175 °C the electron yield is reasonably stable, showing that the macroscopic charging of LiF target can be avoided by increasing the ionic conduction at these temperatures. Recently, Meissl *et al.*[15] have also reported that the target temperature of about 170 °C is sufficient to get rid of the macroscopic target charging during electron yield measurement of LiF. Surprisingly for MgF_2, the measured electron yield did not vary with target temperature. The electron yield of MgF_2 was even more stable at low target temperatures (as indicated in Fig. 3 by the fact that the statistical error in electron yield increases with the increase of the temperature). It has been reported that ionic conduction in alkali halide thin films increases with temperature increasing and it is predominantly due to the conduction of fluorine ions.[18] The fluorine content in MgF_2 greater than that in LiF may be responsible for avoiding the surface charging of MgF_2 even at low temperatures, which results in stable electron yield measurement. Meissl *et al.*[15] have also reported that during the measurement of electron yields of LiF and CaF_2, charging behaviour of LiF is quite different from that of CaF_2. For CaF_2 the ionic conduction starts just at 40 °C as compared with 170 °C for LiF.

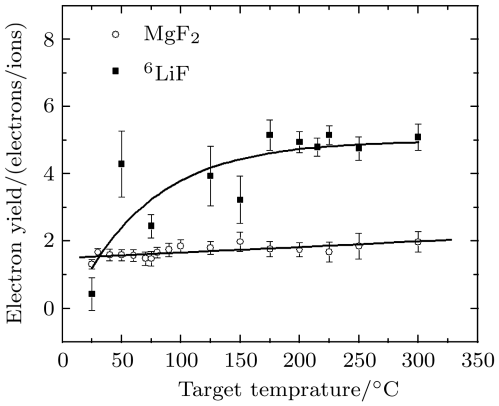


Fig. 3. Temperature dependences of the secondary electron yields from ^{6}LiF and MgF_2 produced by the 8-keV Ar^+ ions.

Figure 4 shows the electron yields of ^{6}LiF and ^{7}LiF for normal impact of 2–10 keV Ar^+ ions. The targets were kept at 300 ± 5 °C during this measurement. The electron yield of ^{7}LiF may be compared with the data from earlier investigations on ^{7}LiF for 5–25 keV[19] and 0.2–8 keV[20] impact of Ar^+ ions. Our result is in agreement with that given by Konig *et*

al.[19] who used a similar current measuring technique. But Vana *et al.*[20] used the electron emission statistic technique to measure higher electron yields particularly at low impact energies. The electron yield of LiF is much large as compared with those of metals.[6] This may be due to the large electron escape depth and to a lower surface barrier potential of LiF, which results in a large escape probability of electrons. Another important finding of this study is that above 4-keV ion energy the electron yield of ^{6}LiF is consistently high as compared with that of ^{7}LiF. Though the electronic structures of ^{6}LiF and ^{7}LiF are identical, their electron yields above 4-keV ion energy are clearly different from those obtained from the kinetic electron emission model (Eq. (1)). The agreement between this model and experiments is generally quite good for light ion bombardment.[9,21,22] But for heavy ions, deviations from the simple rule given by Eq. (1) have been observed for several materials. For example, the experiments by Frischkorn and Groeneveld[23] for C^+ and O^+ impact on C,[23] Jacobsson and Holmén[22] for Ar^+, Kr^+ and Xe^+ impact on SiO_2, Rothard *et al.*[24] for C^+, and O^+ impact on Cu, and Svensson *et al.*[25] for Ar^+ and Xe^+ impact on Al showed that kinetic electron yields increased more slowly with S_e than predicted by Eq. (1). It has been suggested by these authors that for heavier projectile ions having keV energies, a sizeable contribution to electron emission is due to the energy deposited by the recoiling target atoms in the solid. Recently, Ohya[26,27] and Ullah *et al.*[28] have estimated the yields of secondary electrons generated by recoiling target atoms for heavy ion impact on Al, SiO_2 and MgO targets respectively by using the Monte Carlo computer program. The electronic energy losses of ions and mean free paths of electrons in ^{6}LiF and ^{7}LiF are the same. Similarly, the surface work functions of both targets are also identical. Therefore, the observed difference in electron yield between ^{6}LiF and ^{7}LiF is most probably related to the dissimilar contributions of secondary electrons generated by the recoiling ^{6}Li and ^{7}Li atoms. This explanation is based on the fact that ^{6}LiF has a greater nuclear stopping power than those of ^{7}LiF for Ar^+ ions. Figure 5(a) shows the plots of nuclear stopping powers calculated by computer code SRIM 2008.[29] At low ion energies (i.e. less than 4 keV), where the difference in nuclear stopping between ^{6}LiF and ^{7}LiF is not so much, the expected small difference in electron yield between these targets could not be detected.

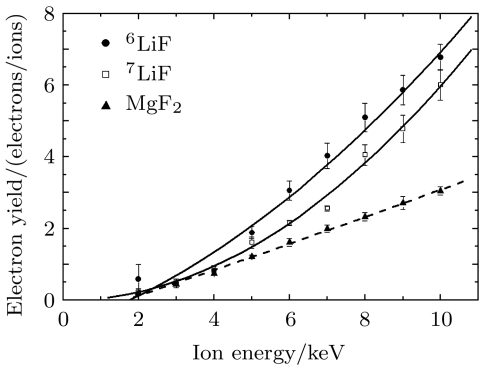


Fig. 4. Secondary electron yields of ^{6}LiF, ^{7}LiF and MgF_2 thin films each as a function of Ar^+ energy.

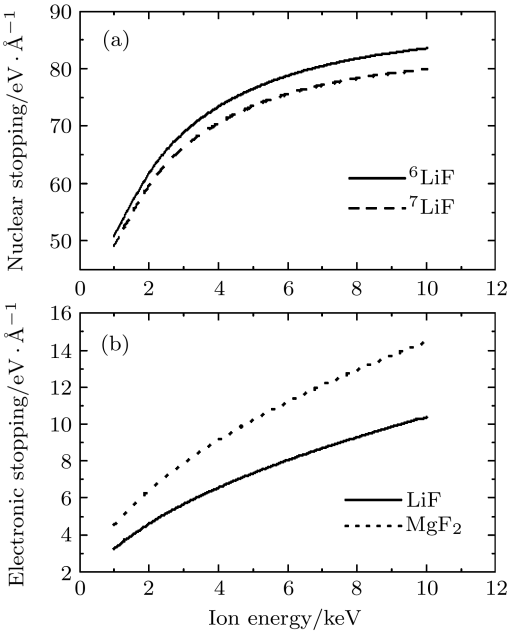


Fig. 5. (a) Nuclear stopping powers of ^{6}LiF and ^{7}LiF, and (b) electronic stopping powers of LiF and MgF_2 each as a function of Ar^+ energy.

Figure 4 also shows the electron yield of MgF_2 for normal impact of 2–10 keV Ar^+ ions. Contrary to the electron yield of LiF targets, the electron yield of MgF_2 rises linearly with ions energy increasing. This behaviour is quite similar to that for the metal targets.[6] Another important result of this study is the lower electron yield of MgF_2 than that of LiF, particularly above 4-keV projectile energy. As indicated in Section 1, the kinetic electron emission is of a three-step process, i.e. production of secondary electrons, their transport towards the surface, and transmission through the surface potential barrier. The first step is related mostly to the electronic energy loss of ions in the target with a small but non-negligible contribution from nuclear energy loss. The calculations performed with SRIM 2008 shows that the electronic stopping

power of MgF_2 is considerably higher than that of LiF (see Fig. 5(b)). The surface barrier potential of insulators is usually taken to be equal to its electron affinity χ,[12] because for insulators χ plays a role similar to the ordinary surface barrier, $U = E_F + \Phi$, for metals, where E_F and Φ are the Fermi energy and the work function respectively. The χ values of MgF_2 and LiF respectively are 0.5 eV and 1.0 eV. The higher electronic stopping and the lower surface barrier potential of MgF_2 both predict higher secondary electron yield of MgF_2 than that of LiF, which is in contrast to the experimental results presented in Fig. 4. Regarding the second step that is transport of secondary electrons towards the surface, the inelastic mean free paths (IMFPs) of electrons in MgF_2 and LiF were calculated by using Tanuma, Powell, Penn (TPP-2M) predictive formula[30] and are given in Fig. 6. For the electron energy range (< 100 eV), which is relevant to this study, the inelastic mean free paths of electrons in MgF_2 are about 1.5 to 2 times shorter than those in LiF. Due to short inelastic mean free paths a large fraction of secondary electron cannot reach the MgF_2 surface. Therefore, the short IMFP of electrons in MgF_2 can be one of the reasons for its lower secondary electron yield than that of LiF. At low projectile energies the electron yields of both targets are almost the same (see Fig. 4) because in this case most of the secondary electrons have their origins close to surface and as a result their IMFPs cannot make much difference in secondary electron yield between MgF_2 and LiF.

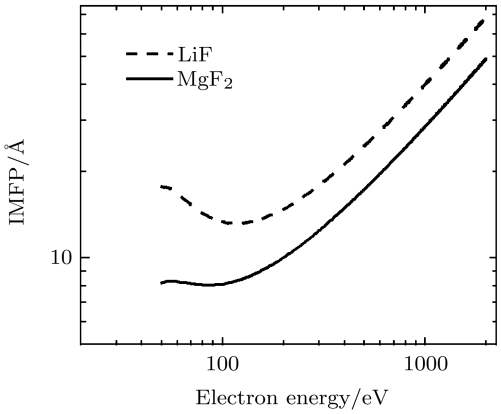


Fig. 6. Ineleastic mean free paths (IMFPs) of secondary electrons in LiF and MgF_2 each as a function of electron energy. IMEPs are calculated by using TPP-2M predictive formula.[30]

In summary, we have measured ion-induced electron yields of ^{6}LiF, ^{7}LiF and MgF_2 thin films by using a current measuring technique. Remarkably dissimilar target temperature effects on the electron yields of LiF and MgF_2 films have been reported and compared with the existing data. This novel feature deserves further investigation. By comparing the electron yields of ^{6}LiF and ^{7}LiF the clear evidence of the secondary electrons generated by recoiling target atoms has been provided. The observed difference in electron yield between MgF_2 and LiF has been explained in terms of the inelastic mean free path of electrons in these materials. Similar work on several other alkali halides is in progress.

Acknowledgment

We are thankful to professor Friedrich Aumayr (Technische Universität Wien) for the helpful suggestions on the data.

References

[1] Sternglass E J 1957 *Phys. Rev.* **108** 1
[2] Hasselkamp D 1992 *Particle Induced Electron Emission II* (Heidelberg: Springer) p. 112
[3] Schou J 1980 *Phys. Rev.* B **22** 2141
[4] Baragiola R A, Alonso E A and Oliva-Florio A 1979 *Phys. Rev.* B **19** 121
[5] Baragiola R A, Alonso E A, Ferron J and Oliva-Florio A 1979 *Sur. Sci.* **90** 240
[6] Alonso E A, Baragiola R A, Ferrón J, Jakas M M and Oliva-Florio A 1980 *Phys. Rev.* B **22** 80
[7] Lakits G, Aumayr F and Winter H P 1989 *Rev. Sci. Instr.* **60** 3151
[8] Cernusca S, Fürsatz M, Winter H P and Aumayr F 2005 *Europhys. Lett.* **70** 768
[9] Rothard H, Kroneberger K, Veje E, Clouvas A, Lorenzen P, Keller N, Kemmler J, Meckbach W and Groeneveld K O 1990 *Phys. Rev.* A **41** 2521
[10] Hasselkamp D, Lang K G, Scharmann A and Stiller N 1981 *Instr. Method* **180** 349
[11] Hosaka K, Matsunami N and Tawara H 1999 *Instr. Method* B **149** 414
[12] Lee S K, Kim J H, Lee J and Whang K W 2003 *Thin Solid Films* **435** 69
[13] Riccardi P, Ishimoto M, Barone P and Baragiola R A 2004 *Surf. Sci.* **571** L305

[14] Stöckl J, Suta T, Ditori F, Winter H P and Aumayr F 2004 *Phys. Rev. Lett.* **93** 263201
[15] Meissl W, Winklehner D, Aumayr F, Simon M C, Ginzel R, López J R C, Ullrich J, Solleder B, Lemel C and Burgdörfer J 2008 *e-J. Surf. Sci. Nanotech.* **6** 54
[16] Dogar A H, Ullah S and Qayyum A 2007 *Nucl. Instr. Method* B **260** 525
[17] Eder H, Messerschmidt W, Winter H P and Aumayr F 2000 *J. Appl. Phys.* **87** 8198
[18] Kawamoto Y, Kanno R and Fujiwara J 1991 *J. Mater. Sci. Lett.* **10** 804
[19] Konig W, Krebs K and Rogaschewski S 1975 *Int. J. Mass Spectrom.* **16** 243
[20] Vana M, Aumayr F, Varga P and Winter H P 1995 *Nucl. Instr. Method* B **100** 284
[21] Benka O, Steinbauer E and Bauer P 1994 *Nucl. Instr. Method* B **90** 64
[22] Jacobsson H and Holmén G 1994 *Phys. Rev.* B **49** 1789
[23] Frischkorn H J and Groeneveld K O 1983 *Phys. Scripta* **T6** 89
[24] Rothard H, Kroneberger K, Burkhard M, Kemmler J, Koschar P, Heil O, Biedermann C, Lencinas S, Keller N, Lorenzen P, Hofmann D, Clouvas A, Groeneveld K O and Veje E 1989 *Radiation Effects and Defects in Solids* **109** 281
[25] Svensson B and Holmén G 1981 *J. Appl. Phys.* **52** 6928
[26] Ohya K 2002 *Nucl. Instr. Method* B **195** 281
[27] Ohya K and Ishitani T 2004 *Appl. Sur. Sci.* **237** 606
[28] Ullah S, Dogar A H and Qayyum A 2008 *Eur. Phys. J. Appl. Phys.* **44** 235
[29] Ziegler J F *SRIM 2008* http://www.srim.org/
[30] Tanuma S, Powell C J and Penn D R 1994 *Surf. Interface Anal.* **21** 165